

# Calcined Bean Dregs-Hydrocalumite Composites as Efficient Adsorbents for the Removal of Ofloxacin

Haohui Zhang, Xi Zhou,\* and Deyi Luo

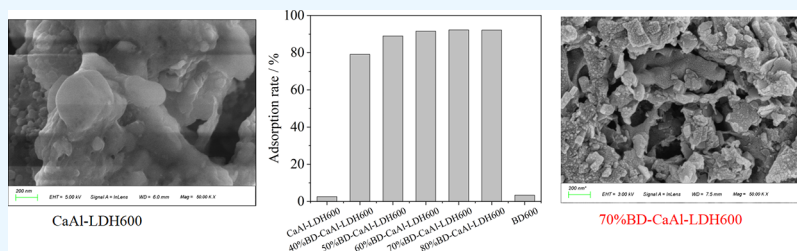
Cite This: *ACS Omega* 2023, 8, 49191–49200

Read Online

ACCESS |

Metrics &amp; More

Article Recommendations



**ABSTRACT:** Calcined bean dregs-hydrocalumite composites were prepared through in situ self-assembly of hydrocalumite on the surface of bean dregs and used for the adsorption of ofloxacin from water. The adsorbents were characterized by scanning electron microscopy, X-ray powder diffraction, and  $N_2$  physical adsorption. The results showed that the adsorption performance of calcined bean dregs-hydrocalumite composites for ofloxacin was much better than that of a single bean dreg carbon or calcined hydrocalumite. The effects of preparation and adsorption conditions on the adsorption property of calcined bean dregs-hydrocalumite for ofloxacin were also investigated. The adsorption ratio of ofloxacin reached up to 99.93% using  $4 \text{ g}\cdot\text{L}^{-1}$  adsorbent dosage with  $20 \text{ mg}\cdot\text{L}^{-1}$  initial concentration of ofloxacin at  $30^\circ\text{C}$  in 2 h. The adsorption process mainly occurred in the first 5 min. In addition, the adsorption of ofloxacin by calcined bean dregs-hydrocalumite was more in line with pseudo-second-order dynamics and the Langmuir isotherm model.

## INTRODUCTION

Antibiotics are widely used in industries such as human disease treatment and animal husbandry. Antibiotic properties are relatively stable, hard to metabolize, and generally with waste being directly deposited in the water environment. With increasing antibiotic usage, frequent from a natural water environment to detect antibiotic residues, causing serious pollution to the environment.<sup>1–3</sup> Thus, solving the pollution problem of antibiotics in the water environment has important significance.<sup>4</sup>

At present, the removal methods of antibiotics and other organic pollutants include adsorption,<sup>5</sup> chemical oxidation,<sup>6</sup> photocatalysis,<sup>7</sup> biodegradation,<sup>8</sup> encapsulation,<sup>9</sup> and other methods. Among them, the adsorption method has received much attention for its advantages of high efficiency, low cost, and simple operation. Many adsorbents for antibiotics have been reported,<sup>10–19</sup> such as carbon materials,<sup>10</sup> molecular sieves,<sup>11</sup> metal–organic framework materials,<sup>12</sup> and hydroxalite-like materials.<sup>13–19</sup> Hydroxalites, also known as layered double hydroxides (LDHs), consists of layered stacks, similar to the layered layers of the mineral brucite  $\text{Mg}(\text{OH})_2$ , and other variants can also be synthesized by replacing cations with other divalent cations (for example,  $\text{Mg}^{2+}$ ,  $\text{Co}^{2+}$ ,  $\text{Ni}^{2+}$ , and  $\text{Zn}^{2+}$ ) and trivalent cations (for example,  $\text{Al}^{3+}$ ,  $\text{Fe}^{3+}$ ,  $\text{Cr}^{3+}$ ,  $\text{Ga}^{3+}$ ), and anions located in the interlamellar region can also be

altered by other inorganic and organic anions. It has a special case where the divalent ions ( $\text{M}^{2+}$ ) of the layered layer are occupied by  $\text{Ca}^{2+}$  ions, and this type of material is called calcium aluminum hydroxalite, and its general formula is  $[\text{Ca}_2\text{M}^{3+}(\text{OH})_6]^+[(\text{A}^{n-})_{(1/n)}\cdot m\text{H}_2\text{O}]^-$ . In the hydroxalite, the trivalent cations in the lamellar is  $\text{Al}^{3+}$ .<sup>13</sup> Sharma et al. designed and synthesized a novel porous Zn/Fe layered double hydroxide and found that it performs high adsorption capacity for ciprofloxacin.<sup>14</sup> Qiu et al. prepared a Mg/Fe layered double hydroxide and used it for the absorption of norfloxacin. When the molar ratio of Mg/Fe is 5:1, it had the optimal adsorption performance for  $20 \text{ mg}\cdot\text{L}^{-1}$  NOR.<sup>15</sup>

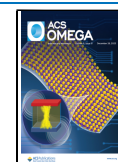
To further improve the adsorption performance of LDHs, the researchers tried to combine biochar with LDHs to prepare a composite adsorbent with better adsorption performance for antibiotics.<sup>17–19</sup> For example, Hoang et al. prepared a novel bagasse biochar/ZnAl-layered double hydroxide by in situ

Received: September 27, 2023

Revised: November 26, 2023

Accepted: November 29, 2023

Published: December 13, 2023



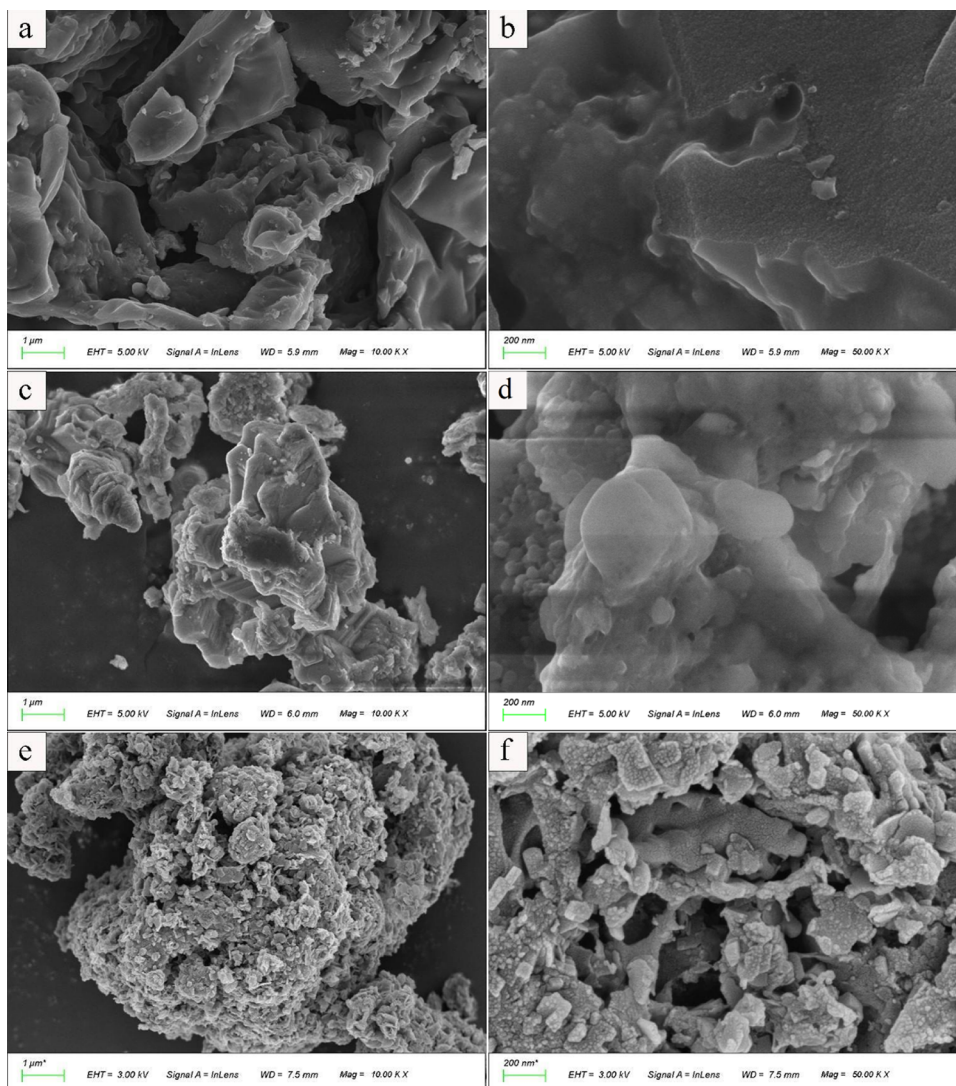


**Figure 1.** SEM micrographs of BD600 (a, b), CaAl-LDH600 (c, d), and 70% BD-CaAl-LDH600 (e and f).

growth and used it for the adsorption removal of tetracycline in water. The results showed that the maximum adsorption capacity of tetracycline by the composite reaches  $41.98 \text{ mg}\cdot\text{g}^{-1}$ , which is much better than that of  $9.82 \text{ mg}\cdot\text{g}^{-1}$  of bagasse biochar.<sup>17</sup> Zheng et al. used sludge biochar-loaded hydrotalcite as the composite adsorbent to effectively remove the low concentration of ciprofloxacin. The adsorption capacity of the composite adsorbent to ciprofloxacin was  $14 \text{ mg}\cdot\text{g}^{-1}$ , which was 2.8 times that of sludge biochar.<sup>19</sup>

Compared with the above hydrotalcite, hydrocalumite has the advantages of lower production cost and environmental friendliness.<sup>20</sup> Bean dregs are the main byproduct of the soybean product processing industry. Bean dregs have been used to adsorb and remove pollutants such as dyes, heavy metals, and pesticides in water.<sup>20–23</sup> However, there have been no reports on the adsorption of antibiotics by bean dregs. Herein, calcined bean dregs-hydrocalumite composite adsorbents were prepared by the self-assembly of hydrocalumite on the surface of bean dregs and subsequent calcination. Ofloxacin, an important antibiotic, was used as a model molecule to study the adsorption properties of bean dregs carbon-calcined hydrocalumite. The results showed that the adsorption performance of calcined bean dregs-hydrocalumite

composites for ofloxacin is much better than that of a single bean dregs carbon or calcined hydrocalumite. It provides a feasible new approach for the development of efficient composite adsorption materials for the adsorption of antibiotics in water.

## RESULTS AND DISCUSSION

**Material Characterization and Analysis.** The surface morphology of BD600, CaAl-LDH600, and 70% BD-CaAl-LDH600 was characterized by scanning electron microscopy (SEM), and the results are shown in Figure 1. BD600 Figure 1a,b showed irregular blocky shapes with a small number of relatively large pores and a relatively smooth surface. CaAl-LDH600 Figure 1c,d showed a layered stacking structure, with a smooth surface and obvious aggregation phenomenon. Compared with BD600 and CaAl-LDH600, the surface topography of 70% BD-CaAl-LDH600 (Figure 1e,f) exhibited significant changes, with a rough surface filled with wrinkles and pores. The reason might be that the crystal of hydrocalumite grown in situ on the cellulose skeleton of bean dregs in the process of preparing 70% BD-CaAl-LDH600, making the crystal of hydrocalumite have good dispersion on the surface of bean dregs and less prone to aggregation.<sup>20</sup>

Therefore, a morphology structure favorable for ofloxacin adsorption was formed, as shown in Figure 1e,f.

X-ray diffraction (XRD) was used to characterize BD600, CaAl-LDH, CaAl-LDH600, and 70% BD-CaAl-LDH600. As shown in Figure 2, the wide and low typical diffraction peak

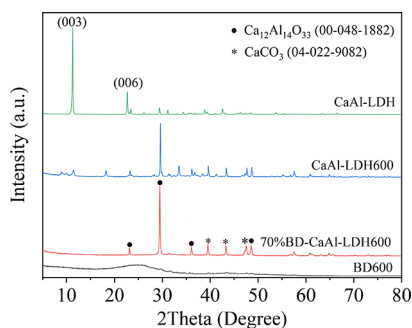


**Figure 2.** XRD patterns of CaAl-LDH, BD600, CaAl-LDH600, and 70% BD-CaAl-LDH600.

near  $25^\circ$  is the symbol of amorphous carbon in the XRD pattern of BD600.<sup>24</sup> The peaks at  $11.2^\circ$  and  $23.3^\circ$  in the spectrum of CaAl-LDH are the (003) and (006) crystal plane diffractions of the typical double-layer structure of hydroxalcalcite. These two peaks almost disappeared in the XRD spectra of CaAl-LDH600 and 70% BD-CaAl-LDH600, indicating the disappearance of the layered structure, which is similar to the results reported in the literature.<sup>25</sup> In the spectrum of 70% BD-CaAl-LDH600,  $23.1^\circ$ ,  $29.5^\circ$ ,  $36.1^\circ$ , and  $48.6^\circ$  are the characteristic diffraction peaks of calcium–aluminum composite oxides such as  $\text{Ca}_{12}\text{Al}_{14}\text{O}_{33}$ , and  $39.5^\circ$ ,  $43.3^\circ$ , and  $47.5^\circ$  are the characteristic diffraction peaks of  $\text{CaCO}_3$ , which indicates that the composite contains calcium–aluminum composite oxide and  $\text{CaCO}_3$ .<sup>20,26,27</sup> In addition, no diffraction peaks of amorphous carbon was found in the 70% BD-CaAl-LDH600, indicating that bean dregs carbon exhibits good dispersion, and most of the bean dregs carbon may be wrapped by calcined hydroxalcalcite.<sup>28</sup>

The specific surface area ( $S_{\text{BET}}$ ), pore size distribution, and pore volume were tested by  $\text{N}_2$  physical adsorption methods, and the result is shown in Figure 3 and Table 1. The  $S_{\text{BET}}$  of 70% BD-CaAl-LDH600 ( $17.784 \text{ m}^2\cdot\text{g}^{-1}$ ) was about 1.8 and 2.2 times that of BD600 ( $9.81 \text{ m}^2\cdot\text{g}^{-1}$ ) and CaAl-LDH600 ( $8.100 \text{ m}^2\cdot\text{g}^{-1}$ ), respectively. The pore volumes of BD600, CaAl-LDH600, and 70% BD-CaAl-LDH600 were 0.031, 0.031, and  $0.114 \text{ cm}^3\cdot\text{g}^{-1}$ , respectively. The above results showed that the  $S_{\text{BET}}$  and pore volume of 70% BD-CaAl-LDH600 were much

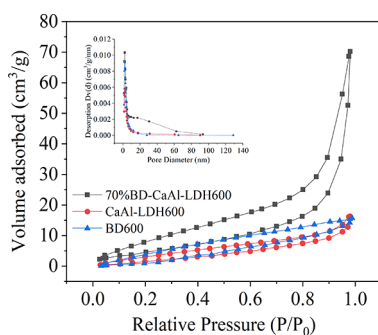


**Figure 3.**  $\text{N}_2$  physical adsorption–desorption isotherms of BD, CaAl-LDH600, and 70% BD-CaAl-LDH600.

**Table 1.**  $S_{\text{BET}}$ , Pore Size, and Pore Volume of the Adsorbent

adsorbent	$S_{\text{BET}}$ ( $\text{m}^2\cdot\text{g}^{-1}$ )	pore size (nm)	pore volume ( $\text{cm}^3\cdot\text{g}^{-1}$ )
BD600	9.811	2.745	0.0310
CaAl-LDH600	8.100	1.921	0.0310
70% BD-CaAl-LDH600	17.78	1.935	0.114

more than those of BD600 and CaAl-LDH600. Therefore, 70% BD-CaAl-LDH600 might be more appropriate as an efficient adsorption material, which was consistent with the SEM results from Figure 1.

**Evaluation of Adsorption Properties.** *Effect of Adsorbents on the Adsorption of Ofloxacin.* The effects of BD600, CaAl-LDH600, and 70% BD-CaAl-LDH600 on the adsorption performance for ofloxacin were investigated under the conditions of  $20 \text{ mg}\cdot\text{L}^{-1}$  ofloxacin initial concentration,  $2 \text{ g}\cdot\text{L}^{-1}$  adsorbent dosage,  $30^\circ\text{C}$ , and 2 h. As shown in Figure 4,

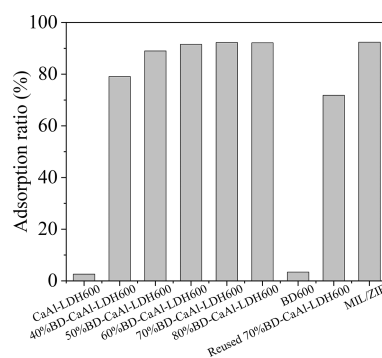


**Figure 4.** Effects of different adsorbents on the adsorption ratio of ofloxacin under the conditions of the initial concentration of ofloxacin  $20 \text{ mg}\cdot\text{L}^{-1}$ , adsorption temperature of  $30^\circ\text{C}$ , adsorption time of 2 h, and adsorbent dosage of  $2 \text{ g}\cdot\text{L}^{-1}$ .

the adsorption ratio of BD600 and CaAl-LDH600 to ofloxacin was only 3.39 and 2.59%, respectively. However, the adsorption ratio of 70% BD-CaAl-LDH600 to ofloxacin was as high as 92.24%. The above results showed that the adsorption performance of 70% BD-CaAl-LDH600 for ofloxacin was significantly better than that of single BD600 and CaAl-LDH600. Combining the characterization results of SEM Figure 1 and  $\text{N}_2$  physical adsorption Table 1, the surface of 70% BD-CaAl-LDH600 was rougher than BD600 and CaAl-LDH600, and it was filled with wrinkles and pores. In addition, the  $S_{\text{BET}}$  and pore volume of 70% BD-CaAl-LDH600 were much more than those of BD600 and CaAl-LDH600. Therefore, 70% BD-CaAl-LDH600 could provide more active sites for the adsorption of ofloxacin, which might be the reason for its better adsorption performance.

To clarify the structure–activity relationship of calcined bean dregs-hydroxalcalumite composites, the effects of bean dregs dosage on the adsorption performance of composites for ofloxacin were also investigated; the results are shown in Figure 4. The adsorption ratio increased from 79.11 to 92.24% with an increase in the amount of bean dregs (based on the total mass of adsorbent) from 40 to 70%. The amount of bean dregs was continuously increased to 80%, and the adsorption ratio exhibited no significant change. Combined with the characterization results, the introduction of bean dregs can provide an attachment matrix material for the nucleation and

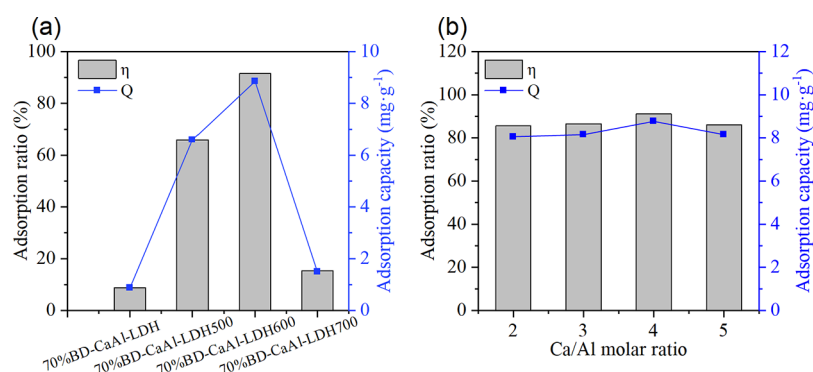


**Figure 5.** Effects of adsorbents synthesized with different calcination temperatures (a) and Ca/Al molar ratios (b) on the adsorption ratio of ofloxacin under the conditions of initial concentration of ofloxacin  $20 \text{ mg}^{-1}$ , adsorption temperature of  $30 \text{ }^{\circ}\text{C}$ , adsorption time of 2 h, and adsorbent dosage of  $2 \text{ g}\cdot\text{L}^{-1}$ .

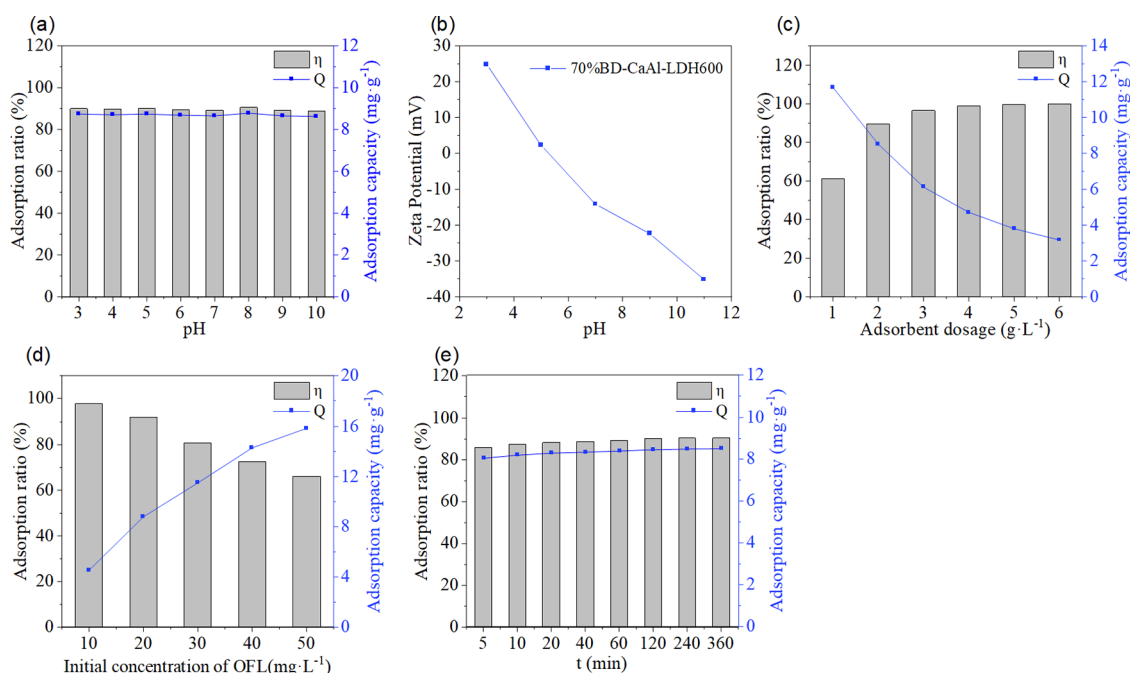


**Figure 6.** Effects of different pH (a) on the adsorption ratio of ofloxacin under the conditions of initial concentration of ofloxacin  $20 \text{ mg}\cdot\text{L}^{-1}$ , adsorption temperature of  $30 \text{ }^{\circ}\text{C}$ , adsorption time of 2 h, and adsorbent dosage of  $2 \text{ g}\cdot\text{L}^{-1}$ . Zeta potentials (b) of 70% BD-CaAl-LDH600 at different pH. The effects of different adsorbent dosage (c) on the adsorption ratio of ofloxacin under the conditions of initial concentration of ofloxacin  $20 \text{ mg}\cdot\text{L}^{-1}$ , adsorption temperature of  $30 \text{ }^{\circ}\text{C}$ , and adsorption time of 2 h. The effects of the initial concentration of ofloxacin (d) on the adsorption ratio of ofloxacin under the conditions of adsorption temperature of  $30 \text{ }^{\circ}\text{C}$ , adsorption time of 2 h, and adsorbent dosage of  $2 \text{ g}\cdot\text{L}^{-1}$ . The effects of different adsorption time (e) on the adsorption ratio of ofloxacin under the conditions of initial concentration of ofloxacin  $20 \text{ mg}\cdot\text{L}^{-1}$ , adsorption temperature of  $30 \text{ }^{\circ}\text{C}$ , and adsorbent dosage of  $2 \text{ g}\cdot\text{L}^{-1}$ .

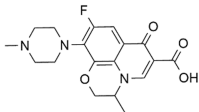
growth of hydrocalumite crystals, which is conducive to the dispersion of hydrocalumite and avoids aggregation. After calcining, rough, porous, and high-specific surface adsorption materials that are conducive to adsorbing ofloxacin can be formed. When the amount of bean dregs is excessive, the proportion of calcined hydrocalumite components in the composites is too small, and it is difficult to continue to improve its adsorption ratio. In addition, in the process of preparing composite adsorption materials, the addition of excessive bean dregs will lead to difficult filtration and separation of products, which will affect the preparation efficiency and cost. Therefore, the optimal amount of bean dregs is 70%.

As shown in Figure 4, 70% BD-CaAl-LDH600 could be reused after calcining under the same calcining conditions as

synthesis, and the adsorption ratio was 71.28% after four regeneration cycles; 70% BD-CaAl-LDH600 exhibited adsorption performance comparable to the highly efficient adsorption materials reported in the literature, such as MIL-53(Fe) and ZIF-8.<sup>29</sup>

*Effect of Calcination Temperature on the Adsorption Performance of Calcined Bean Dregs-Hydrocalumite for Ofloxacin.* According to literature reports,<sup>20,30–32</sup> the calcination temperature has a significant effect on the adsorption performance of biochar and calcined hydrocalumite adsorbents. Therefore, the effect of calcination temperature on the adsorption performance of calcined bean dregs-hydrocalumite for ofloxacin was investigated under the conditions of initial ofloxacin concentration of  $20 \text{ mg}\cdot\text{L}^{-1}$ , adsorbent dosage of  $2 \text{ g}\cdot\text{L}^{-1}$ , adsorption temperature of  $30 \text{ }^{\circ}\text{C}$ , and adsorption time of 2

Table 2. Molecular Structure of Ofloxacin

Name	Adsorbates	pK <sub>a1</sub>	pK <sub>a2</sub>	Molecular weight	Structure
Ofloxacin	OFL	5.98	8.00	361	

h. According to the results of Figure 5a, the adsorption ratio of ofloxacin by 70% BD-CaAl-LDH was only 8.72%. The adsorption ratio of ofloxacin by 70% BD-CaAl-LDH500 prepared by calcining at 500 °C was greatly increased to 65.81%, indicating that the calcining process was conducive to improving its adsorption performance. When the calcining temperature was increased to 600 °C, the adsorption ratio of ofloxacin by 70% BD-CaAl-LDH600 was further increased to 92.24%. Further increasing the calcination temperature to 700 °C, the adsorption ratio showed a significant decrease. The reason might be that the appropriate calcination temperature is conducive to the formation of porous, high specific surface calcined bean dregs-hydrocalumite composite material, and too high calcination temperature will lead to the collapse of pores and the accumulation of particles, which in turn leads to a decrease in adsorption performance.<sup>31,33</sup> Therefore, the appropriate calcination temperature was 600 °C for the preparation of calcined bean dregs-hydrocalumite composite adsorbents.

**Effect of the Ca/Al Molar Ratio on the Adsorption Performance of Calcined Bean Dregs-Hydrocalumite for Ofloxacin.** The ratio of raw materials has a remarkable influence on the structure and crystal growth of hydrocalumite-like materials.<sup>17,20,34,35</sup> The effects of the Ca/Al molar ratio on the adsorption of ofloxacin by calcined bean dregs-hydrocalumite composite material were investigated under the conditions of initial ofloxacin concentration of 20 mg·L<sup>-1</sup>, adsorbent dosage of 2 g·L<sup>-1</sup>, adsorption temperature of 30 °C, and adsorption time of 2 h. As shown in Figure 5b, the adsorption ratio of calcined bean dregs-hydrocalumite composite material increased from 85.53 to 91.03% with the increasing Ca/Al molar ratio of raw materials from 2:1 to 4:1. However, the adsorption ratio of the composite material decreased to 86.08% with further increasing the Ca/Al molar ratio to 5:1. Therefore, the optimum Ca/Al molar ratio of calcined bean dregs-hydrocalumite was 4:1. Through chemical analysis, the actual Ca/Al molar ratio of the optimal calcined bean dregs-hydrocalumite was 4.16:1.

**Effects of Adsorption Conditions on the Adsorption Performance of 70% BD-CaAl-LDH600 for Ofloxacin.** Using 70% BD-CaAl-LDH600 as adsorbent, the effect of adsorption solution pH on the adsorption performance of ofloxacin was investigated under the conditions of initial concentration of 20 mg·L<sup>-1</sup>, adsorbent dosage of 2 g·L<sup>-1</sup>, adsorption temperature of 30 °C, and adsorption time of 2 h. The adsorption solution pH was adjusted by adding 0.1 M HCl or 0.1 M NaOH. As shown in Figure 6a, the adsorption ratio had no significant change with the adsorption solution pH range of 3–10. Generally speaking, because ofloxacin has two pK<sub>a</sub> values (Table 2), its aqueous solution exists in three ionic states. When pH < 5.98, ofloxacin is mainly in the form of cations (OFL<sup>+</sup>); when pH > 8.00, it is mainly in the form of anions (OFL<sup>-</sup>); when it is 5.98, it mainly exists in the form of

zwitterion.<sup>36,37</sup> The zeta potential of 70% BD-CaAl-LDH600 at different pH values is shown in Figure 6b. At pH < 5, electrostatic repulsion occurs between the positively charged surface of the composite and OFL<sup>+</sup> in solution, and at pH > 5, electrostatic repulsion also occurs between the negatively charged surface of the composite and the OFL<sup>-</sup> in solution.<sup>19,38</sup> In summary, electrostatic attraction is not the main adsorption mechanism of 70% BD-CaAl-LDH600 on ofloxacin, and the pH value of the solution is not a key factor affecting the adsorption performance of 70% BD-CaAl-LDH600 against ofloxacin.<sup>39</sup>

Using 70% BD-CaAl-LDH600 as adsorbent, the effect of adsorbent dosage on the adsorption performance of ofloxacin was investigated under the conditions of initial concentration of ofloxacin of 20 mg·L<sup>-1</sup>, 30 °C, and 2 h, and the results were shown in Figure 6c. Increasing the 70% BD-CaAl-LDH600 dosage from 1 to 4 g·L<sup>-1</sup>, the adsorption ratio of ofloxacin increased rapidly from 61.31 to 98.96%, but the adsorption capacity decreased from 11.68 to 4.71 mg·g<sup>-1</sup>. Further increasing the amount of 70% BD-CaAl-LDH600 to 5 g·L<sup>-1</sup>, the adsorption ratio was close to 100%. The above results showed that appropriately increasing the dosage of 70% BD-CaAl-LDH600 is beneficial to improve the adsorption ratio of ofloxacin. Under the set adsorption conditions, it can provide sufficient binding sites for adsorption ofloxacin using 4–5 g·L<sup>-1</sup> of 70% BD-CaAl-LDH600 dosage. However, in order to make the difference in the adsorption ratio of ofloxacin under different adsorption conditions more significant and better explore the influence of adsorption conditions on the ofloxacin adsorption ratio, the 70% BD-CaAl-LDH600 dosage was still selected as 2 g·L<sup>-1</sup> in the subsequent adsorption condition optimization experiment.

Considering the low and different initial concentrations of ofloxacin in an actual water environment, the effect of the initial concentration of ofloxacin on the adsorption of ofloxacin by 70% BD-CaAl-LDH600 in the range of 10–50 mg·L<sup>-1</sup> was investigated under the conditions of 2 g·L<sup>-1</sup> adsorbent dosage, 30 °C, and 2 h. As shown in Figure 6d, the adsorption ratio of ofloxacin decreased from 97.51 to 66.14% with an increase in the initial concentration of ofloxacin from 10 to 50 mg·L<sup>-1</sup>, but the adsorption capacity increased from 4.54 to 15.85 mg·g<sup>-1</sup>. It was consistent with the expected results. As the initial concentration of ofloxacin increases, the probability of contact between the adsorbent and ofloxacin increases. In addition, the larger the difference between the initial concentration of ofloxacin and the concentration of the adsorbent, the stronger the mass transfer driving force and the larger the adsorption capacity. However, the adsorption site provided by the adsorbent is fixed, and an increase in the initial concentration of ofloxacin leads to a decrease in the adsorption ratio.

In addition, the effect of adsorption time on the adsorption of ofloxacin by 70% BD-CaAl-LDH600 was also investigated under the conditions of initial ofloxacin concentration of 20

mg·L<sup>-1</sup>, adsorbent dosage of 2 g·L<sup>-1</sup>, and adsorption temperature of 30 °C. According to the results of Figure 6, the adsorption ratio of ofloxacin only slowly increased from 85.70 to 90.03%, prolonging the adsorption time from 5 to 120 min. Further extending the adsorption time to 360 min, the adsorption ratio had no significant change. It showed that the adsorption time has little effect on the adsorption ratio of ofloxacin under the adsorption conditions investigated, and the adsorption process mainly occurs in the first 5 min. Therefore, the adsorption of 70% BD-CaAl-LDH600 to ofloxacin is fast and stable, which is also in line with the subsequent adsorption dynamics and adsorption isotherm model.

**Adsorption Dynamics.** In order to further study the adsorption ratio and adsorption mechanism of ofloxacin by 70% BD-CaAl-LDH600, the pseudo-first-order dynamics model (1) and pseudo-second-order dynamic model (2) were selected to analyze the adsorption process.<sup>40</sup> The model of the formula is as follows:

$$\ln(Q_e - Q_t) = \ln Q_e - K_1 t \quad (1)$$

$$\frac{t}{Q_t} = \frac{1}{K_2 Q_e^2} + \frac{t}{Q_e} \quad (2)$$

where  $Q_e$  and  $Q_t$  are the adsorption capacity (mg·g<sup>-1</sup>) at adsorption equilibrium and  $t$  (min).  $K_1$  (min<sup>-1</sup>) and  $K_2$  (g·mg<sup>-1</sup>·min<sup>-1</sup>) are the rate constants of the pseudo-first-order dynamic model and pseudo-second-order dynamic model, respectively. The model fit is shown in Figure 7, and the parameters  $Q_e$ ,  $K_1$ , and correlation coefficients ( $R^2$ ) are shown in Table 3.

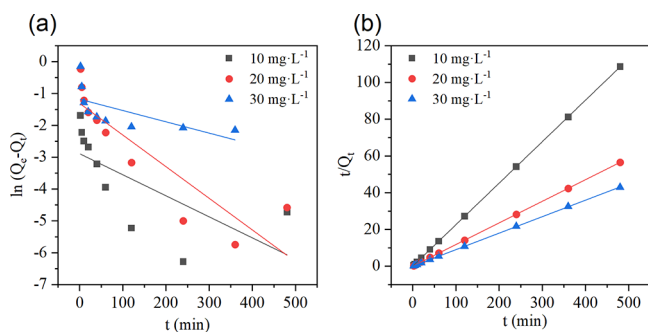


**Figure 7.** Under the conditions that the initial concentration of ofloxacin was 10, 20, 30 mg·L<sup>-1</sup>, the adsorption temperature was 303 K, the amount of adsorbent was 2 g·L<sup>-1</sup>, and the sampling time was 0–480 min, Pseudo-first-order dynamic model (a), pseudo-second-order dynamic model (b) of ofloxacin adsorption by 70% BD-CaAl-LDH600.

According to the dynamic model and fitting parameters for the adsorption of ofloxacin by 70% BD-CaAl-LDH600, the correlation coefficient of the pseudo-second-order dynamic model ( $R^2 > 0.999$ ) was higher than that of the Pseudo-first

order dynamic model ( $R^2 > 0.357$ ). In addition, the theoretical adsorption capacity ( $Q_e$ ) obtained by the pseudo-second order dynamic model was closer to the experimental adsorption capacity ( $Q_{exp}$ ). The results showed that the adsorption process of 70% BD-CaAl-LDH600 on ofloxacin conformed to the pseudo-second-order dynamic model, which was consistent with the kinetic behavior of adsorption reported by Hao et al.<sup>38</sup>

**Adsorption Isotherms.** The adsorption isotherm model can predict the maximum adsorption capacity of the adsorbent and interaction behavior. Therefore, the Langmuir isotherm model (3) and Freundlich isotherm model (4)<sup>41</sup> were selected to analyze the adsorption process of 70% BD-CaAl-LDH600 for ofloxacin. The model of the formula is as follows:

$$\frac{C_e}{Q_e} = \frac{C_e}{Q_m} + \frac{1}{Q_m K_L} \quad (3)$$

$$\ln Q_e = \ln K_F + \frac{1}{n} \ln C_e \quad (4)$$

where  $C_e$  (mg·L<sup>-1</sup>) is the concentration of ofloxacin at adsorption equilibrium.  $Q_e$  (mg·g<sup>-1</sup>) is the equilibrium adsorption capacity of 70% BD-CaAl-LDH600 for ofloxacin;  $Q_m$  (mg·g<sup>-1</sup>) is the theoretical maximum adsorption capacity of 70% BD-CaAl-LDH600 for ofloxacin.  $K_L$ ,  $K_F$ , and  $n$  are the constants of Langmuir, Freundlich, and adsorption strength, respectively.

The isotherms and fitting parameters of adsorption thermodynamics are shown in Figure 8 and Table 4. The

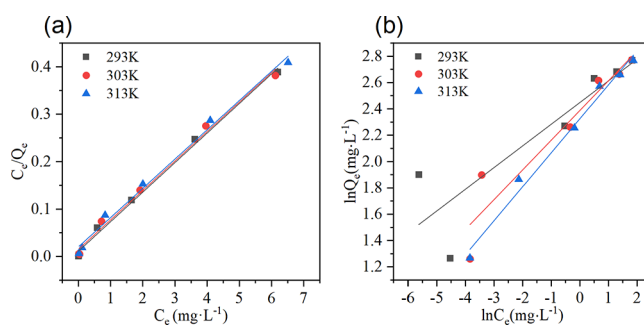


**Figure 8.** Under the conditions that the initial concentration of ofloxacin was 5–30 mg·L<sup>-1</sup>, the adsorption temperature was 293, 303, and 313 K, the amount of adsorbent was 2 g·L<sup>-1</sup>, and the adsorption time was 480 min, Langmuir adsorption isotherm (a) and Freundlich adsorption isotherm (b) of ofloxacin adsorption by 70% BD-CaAl-LDH600.

Langmuir model assumes that adsorption occurs on the surface of a monolayer with the same independent adsorption site as that of the adsorbed particle. The Freundlich isotherm model assumes that adsorption occurs in multiple layers on heterogeneous surfaces.<sup>32</sup> The correlation coefficient fitted to the Langmuir model ( $R^2 > 0.992$ ) was higher than that fitted to

**Table 3.** Fitting Parameters by Pseudo-First-Order and Pseudo-Second-Order Models

$\rho_0$ (mg·L <sup>-1</sup> )	$Q_{exp}$ (mg·g <sup>-1</sup> )	pseudo-first order dynamic model			pseudo-second order dynamic model		
		$K_1$ (min <sup>-1</sup> )	$Q_e$ (mg·g <sup>-1</sup> )	$R^2$	$K_2$ (min <sup>-1</sup> )	$Q_e$ (mg·g <sup>-1</sup> )	$R^2$
10	4.43	2.89	0.465	0.389	1.47	4.427	1.00
20	8.50	1.31	0.789	0.763	0.254	8.503	1.00
30	11.2	1.18	0.437	0.357	0.152	11.15	0.999

**Table 4. Parameters Fitted by the Langmuir and Freundlich Models for Ofloxacin**

$T$ (K)	Langmuir			Freundlich		
	$Q_m$ ( $\text{mg}\cdot\text{g}^{-1}$ )	$K_L$ ( $\text{L}\cdot\text{g}^{-1}$ )	$R^2$	$n$	$K_F$ ( $\text{mg}^{1-n}\cdot\text{L}^n\cdot\text{g}^{-1}$ )	$R^2$
293	89.45	0.0020	0.995	-0.083	0.9201	0.791
303	66.27	0.0037	0.992	-0.104	0.9014	0.905
313	49.04	0.0067	0.992	-0.112	0.8937	0.988

the Freundlich model ( $R^2 > 0.791$ ). The results showed that the adsorption process of 70% BD-CaAl-LDH600 for ofloxacin conforms to the Langmuir adsorption isotherm and occurs on the surface of the monolayer.

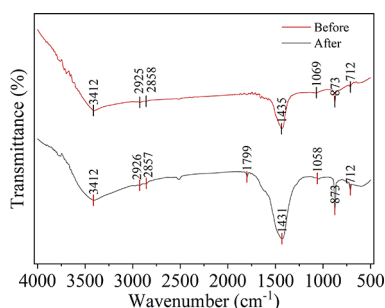
**Comparison of Adsorption Properties.** The adsorption performance of 70% BD-CaAl-LDH600 for ofloxacin was compared with the adsorption materials reported in the literature, and the results are shown in Table 5. The results

**Table 5. Adsorption Properties of 70% BD-CaAl-LDH600 and Other Materials for Ofloxacin**

adsorbent	adsorption capacity ( $\text{mg}\cdot\text{g}^{-1}$ )	temperature ( $^{\circ}\text{C}$ )	ref.
rice husk ash	6.28	25	42
cassava residue-derived biochar	9.68	25	39
modified Ni-Al LDH	8.86		43
calcined magnetic iron nanoparticles	12.80	30	44
ilmenite biochar composite	15.06		45
calcined bean dregs-hydrocalumite composites	15.85	30	present study

showed that the adsorption performance of 70% BD-CaAl-LDH600 for ofloxacin is better than that of similar adsorption materials reported in the literature. In addition, 70% BD-CaAl-LDH600 also has the advantages of cheap raw materials, simple preparation methods, environmental protection, and safety. Therefore, 70% BD-CaAl-LDH600 has good application potential in the field of wastewater adsorption treatment.

**Adsorption Mechanism.** In order to analyze the possible adsorption mechanism of 70% BD-CaAl-LDH600 adsorption of ofloxacin, 70% BD-CaAl-LDH600 samples before and after adsorption of ofloxacin were detected by FT-IR. As the results shown in Figure 9, the peaks at 3412, 2926  $\text{cm}^{-1}$ /2925  $\text{cm}^{-1}$ /2857  $\text{cm}^{-1}$ /2858  $\text{cm}^{-1}$ , 1431  $\text{cm}^{-1}$ /1435  $\text{cm}^{-1}$ , and 1058  $\text{cm}^{-1}$ /1069  $\text{cm}^{-1}$  are the telescopic vibrations of -OH, -C-H, -C=C-O, and -C-O, respectively.<sup>38,46</sup> The peaks

**Figure 9.** FT-IR spectra of 30% BD-LDH before and after adsorption of ofloxacin.

around 873 and 712  $\text{cm}^{-1}$  are caused by the vibration of calcium aluminum oxide.<sup>25,47</sup> After adsorption, the peak at 1799  $\text{cm}^{-1}$  was added compared with before adsorption, where the peak is the characteristic peak of -C=O,<sup>46</sup> representing that the ofloxacin is adsorbed on the surface of the composite.

The results of comprehensive characterization, kinetics, isotherms, and environmental factors showed that the adsorption behavior of ofloxacin on 70% BD-CaAl-LDH600 is a complex reaction involving multiple mechanisms. As shown in Figure 10, the porous structure of 70% BD-CaAl-LDH600 and the large rough surface produce rich active sites for ofloxacin to be adsorbed to 70% BD-CaAl-LDH600, and more oxygen-containing functional groups (-OH, -C-O, and -C=C-O) may also participate in the adsorption of ofloxacin. The mechanism involves complexation, hydrogen bonding, and  $\pi$ - $\pi$  interaction.<sup>18,30,48,49</sup> The adsorption kinetic model proves that the adsorption reaction is mainly physical adsorption, and the isothermal adsorption model shows that the adsorption reaction is mainly physical adsorption and some physical adsorption.<sup>50</sup> The adsorption mechanism of OFL on 70% BD-CaAl-LDH600 mainly includes  $\pi$ - $\pi$  interaction, hydrogen bonding, pore filling, and oxygen-containing functional complexation.

## CONCLUSIONS

The adsorption performance of calcined bean dregs-hydrocalumite composites is significantly better than that of single bean dregs carbon and calcined hydrocalumite for ofloxacin in the aqueous phase. The reason is that the former has a rough surface and a porous structure, with a specific surface area and pore volume about 2 and 3.6 times that of the latter two, respectively. The dosage of bean dregs and the calcination temperature had significant effects on the adsorption performance of composites for ofloxacin. Among the prepared composites, 70% BD-CaAl-LDH600 exhibited the highest adsorption ratio for ofloxacin. Under optimized conditions, the ofloxacin adsorption ratio could reach about 99.93%, and the adsorption process mainly occurred in the first 5 min. The adsorption process of 70% BD-CaAl-LDH600 to ofloxacin was more in line with the pseudo-second-order dynamic model and Langmuir isothermal model. The results provide a feasible new approach for the development of cheap, green, and efficient adsorption materials for the removal of antibiotics, such as ofloxacin, in water.

## EXPERIMENTAL SECTION

**Preparation of Adsorbents.** The pretreatment of the bean dregs was as follows. The fresh bean dregs were washed with water until the filtrate was clear. After drying at 80  $^{\circ}\text{C}$  for 20 h, the solid material was crushed and passed through a 200 mesh sample sieve to obtain the product (marked as BD).

The preparation of the calcined bean dregs-hydrocalumite composite material is shown in Figure 11. BD was added to a three-mouth flask containing 80 mL of water and stirred at high speed to form a homogenate of bean dregs; 18.50 g of  $\text{CaCl}_2$  was added to 120 mL of water to prepare solution A; 3.28 g of  $\text{NaAlO}_2$ , 3.20 g of  $\text{Na}_2\text{CO}_3$ , and 2.40 g of  $\text{NaOH}$  were added to 120 mL of water to form solution B. Then, solutions A and B were simultaneously added dropwise to a three-mouth flask containing bean dregs homogenate at 80  $^{\circ}\text{C}$  and continuous stirring. Stirring was continued for 2 h and then, the mixture was transferred to a crystallization kettle and

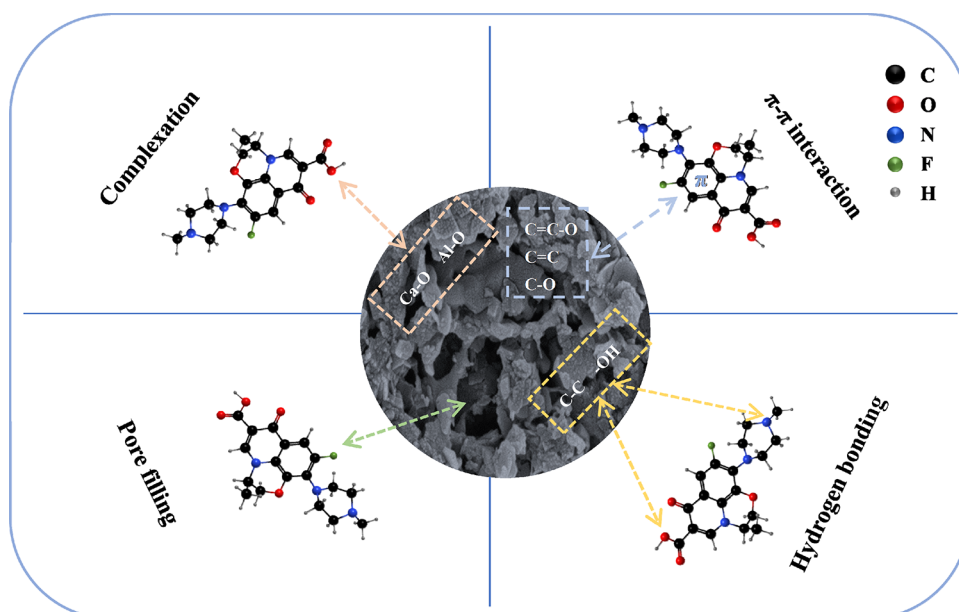


**Figure 10.** Schematic diagram of the adsorption removal mechanism of ofloxacin by 70% BD-CaAl-LDH600.

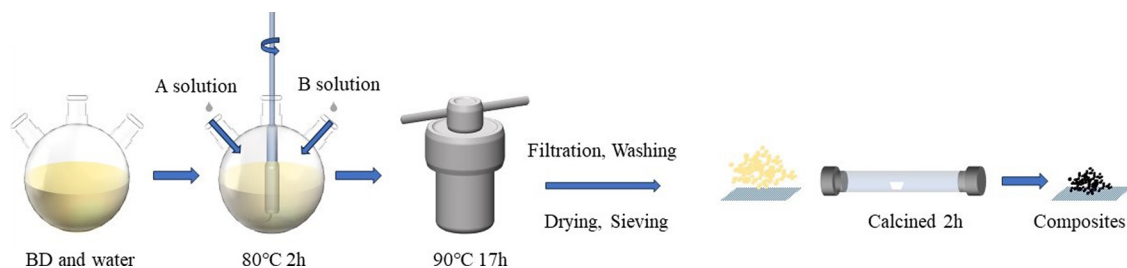


**Figure 11.** Schematic presentation for the synthesis of calcined bean dregs-hydrocalumite composites.

crystallized at 90 °C for 17 h. After the completion of the reaction, the bean dregs-hydrocalumite precursor was prepared by filtration, washing, drying, and crushing through 200 mesh sieve, labeled as  $x\%$  BD-CaAl-LDH, where  $x$  is the bean dregs dosage. The prepared bean dregs-hydrocalumite precursor was put into a vacuum tube furnace, heated at a rate of 10 °C/min, calcined at 500–700 °C for 2 h, and naturally cooled to room temperature to obtain calcined bean dregs-hydrocalumite composite, labeled as  $x\%$  BD-CaAl-LDH $_y$ , where  $y$  is the calcination temperature.

The preparation method of composite materials with different molar ratios: the amount of various reagents was changed according to different Ca/Al molar ratios, and the samples with Ca/Al molar ratios of 2:1, 3:1, 4:1, and 5:1 were prepared according to the same method mentioned above.

The preparation method of CaAl-LDH is the same as that of bean dregs – Ca–Al hydrotalcite composites, except for the absence of soybean residue added, and the calcining method of CaAl-LDH600 is the same as that of  $x\%$ BD-CaAl-LDH $_y$ .

**Characterization of Adsorbents.** The surface morphology of the adsorbent was detected by a scanning electron microscope (SEM, Sigma 300, Zeiss, Germany) with a 3 kV acceleration voltage. The crystal structure of adsorbent was characterized by powder X-ray diffraction (XRD, Bruker D8 Advance, Germany) using the continuous scanning mode of the Cu K $\alpha$  ray ( $\lambda = 0.154056$  nm). The scanning range of  $2\theta$  ranged from 5° to 80°. The physical structure of the adsorbent was tested by the N $_2$  adsorption–desorption method

(Quantachrome Nova 2000e, USA). The specific surface area ( $S_{\text{BET}}$ ) was calculated by the Brunauer–Emmet–Teller equation, and the pore size and volume were calculated by the Barrett–Joyner–Halenda equation. Analysis of functional groups before and after adsorption of ofloxacin by 70% BD-CaAl-LDH600 by Fourier transform infrared spectroscopy (FT-IR, Nicolet iS5, Thermo Fisher, USA) in the range 500–4000  $\text{cm}^{-1}$ .

**Adsorption Performance of Adsorbents.** Ofloxacin (0.0510 g) and 60 mL of purified water were put into a 100 mL volumetric flask, ultrasonicated for 30 min, and cooled to room temperature after complete dissolution, and purified water was used to volume ofloxacin reserve solution. The stock solution was diluted to obtain different concentrations of ofloxacin solutions. Typically, 50 mL of 20  $\text{mg}\cdot\text{L}^{-1}$  ofloxacin solution was transferred into a 250 mL conical flask. After adding 0.1000 g of 70% BD-CaAl-LDH600, the mixture was sealed and placed in a desktop constant temperature oscillator with rotating (200  $\text{r}/\text{min}$ ) at 30 °C for 2 h. After centrifugation, the solid was filtered out using a 0.22  $\mu\text{m}$  filter membrane. The absorbance of the filtrate was determined by spectrophotometry ( $\lambda = 294$  nm), and the residual adsorption concentration was calculated by substituting the standard curve equation  $y = 0.0928x + 0.0105$  ( $R^2 = 0.9999$ ). The adsorption ratio ( $\eta$ ) and adsorption capacity ( $Q$ ) of the adsorbent were calculated by eqs 5 and 6, respectively.



$$n = \frac{\rho_0 - \rho_e}{\rho_0} \times 100\% \quad (5)$$

$$Q = \frac{\rho_0 - \rho_e}{m} \times V \quad (6)$$

where  $\rho_0$  and  $\rho_e$  are the concentration of ofloxacin in the solution before and after adsorption, respectively,  $\text{mg}\cdot\text{L}^{-1}$ ;  $m$  is the mass of adsorbent, g;  $V$  is the volume of ofloxacin solution, L.

## AUTHOR INFORMATION

### Corresponding Author

Xi Zhou – Department of Food and Chemical Engineering, Shaoyang University, Shaoyang, Hunan 422000, PR China; [orcid.org/0009-0004-3262-8203](https://orcid.org/0009-0004-3262-8203); Email: [zhouxi@hnsyu.edu.cn](mailto:zhouxi@hnsyu.edu.cn)

### Authors

Haohui Zhang – Department of Food and Chemical Engineering, Shaoyang University, Shaoyang, Hunan 422000, PR China

Deyi Luo – Department of Food and Chemical Engineering, Shaoyang University, Shaoyang, Hunan 422000, PR China

Complete contact information is available at:

<https://pubs.acs.org/10.1021/acsomega.3c07473>

### Notes

The authors declare no competing financial interest.

## ACKNOWLEDGMENTS

This work was funded by supported by the Scientific Research Foundation of Hunan Provincial Education Department of China (19A444) and the Postgraduate Research and Innovation Project in Hunan Province, China (CX20221308).

## REFERENCES

- (1) Danner, M. C.; Robertson, A.; Behrends, V.; Reiss, J. Antibiotic pollution in surface fresh waters: Occurrence and effects. *Sci. Total Environ.* **2019**, *664*, 793–804.
- (2) Huang, J.; He, P.; Duan, H.; Yang, Z.; Zhang, H.; Lu, F. Leaching risk of antibiotic resistance contamination from organic waste compost in rural areas. *Environ. Pollut.* **2023**, *320*, No. 121108.
- (3) Yuan, X.; Lv, Z.; Zhang, Z.; Han, Y.; Liu, Z.; Zhang, H. A Review of Antibiotics, Antibiotic Resistant Bacteria, and Resistance Genes in Aquaculture: Occurrence, Contamination, and Transmission. *Toxics* **2023**, *11* (5), 420.
- (4) Sun, S.; Shen, J.; Li, D.; Li, B.; Sun, X.; Ma, L.; Qi, H. A new insight into the ARG association with antibiotics and non-antibiotic agents-antibiotic resistance and toxicity. *Environ. Pollut.* **2022**, *293*, No. 118524.
- (5) Mangla, D.; Annu, Sharma, A.; Ikram, S. Critical review on adsorptive removal of antibiotics: Present situation, challenges and future perspective. *J. Hazard. Mater.* **2022**, *425*, No. 127946.
- (6) Yuan, Q.; Qu, S.; Li, R.; Huo, Z.-Y.; Gao, Y.; Luo, Y. Degradation of antibiotics by electrochemical advanced oxidation processes (EAOPs): Performance, mechanisms, and perspectives. *Sci. Total Environ.* **2023**, *856*, No. 159092.
- (7) Umar, M. From Conventional Disinfection to Antibiotic Resistance Control-Status of the Use of Chlorine and UV Irradiation during Wastewater Treatment. *Int. J. Environ. Res. Public Health* **2022**, *19* (3), No. 19031636.
- (8) Sun, S.; Geng, J.; Ma, L.; Sun, X.; Qi, H.; Wu, Y.; Zhang, R. Changes in antibiotic resistance genotypes and phenotypes after two typical sewage disposal processes. *Chemosphere* **2022**, *291*, No. 132833.
- (9) Zeng, S.; Tan, J.; Xu, X.; Huang, X.; Zhou, L. Facile synthesis of amphiphilic peach gum polysaccharide as a robust host for efficient encapsulation of methylene blue and methyl orange dyes from water. *Int. J. Biol. Macromol.* **2020**, *154*, 974–980.
- (10) Pan, M. Biochar Adsorption of Antibiotics and its Implications to Remediation of Contaminated Soil. *Water Air Soil Pollut.* **2020**, *231*, 221.
- (11) Al-Jubouri, S. M.; Al-Jendeel, H. A.; Rashid, S. A.; Al-Batty, S. Antibiotics adsorption from contaminated water by composites of ZSM-5 zeolite nanocrystals coated carbon. *J. Water Process Eng.* **2022**, *47*, No. 102745.
- (12) Du, C.; Zhang, Z.; Yu, G.; Wu, H.; Chen, H.; Zhou, L.; Zhang, Y.; Su, Y.; Tan, S.; Yang, L.; et al. A review of metal organic framework (MOFs)-based materials for antibiotics removal via adsorption and photocatalysis. *Chemosphere* **2021**, *272*, No. 129501.
- (13) Yong, W.; Minghao, J.; Yilin, W.; Jingting, X.; Shuo, Z. Advance in construction of layered double hydroxides and their treatment with antibiotics in water. *Chem. Ind. Eng. Prog.* **2022**, *41* (02), 803–815.
- (14) Sharma, S.; Sharma, G.; Kumar, A.; Dhiman, P.; AlGarni, T. S.; Naushad, M.; Allothman, Z. A.; Stadler, F. J. RETRACTED: Controlled synthesis of porous Zn/Fe based layered double hydroxides: Synthesis mechanism, and ciprofloxacin adsorption. *Sep. Purif. Technol.* **2021**, *278*, No. 119481.
- (15) Qiu, Z.; Lin, Q.; Lin, J.; Zhang, X.; Wang, Y. Regenerable Mg/Fe bimetallic hydroxide for remarkable removal of low-concentration norfloxacin from aqueous solution. *Colloids Surf., A* **2022**, *644*, No. 128825.
- (16) Qi, L.; Liu, K.; Wang, R.; Li, J.; Zhang, Y.; Chen, L. Removal of Chlorine Ions from Desulfurization Wastewater by Modified Fly Ash Hydrocalcite. *ACS Omega* **2020**, *5* (49), 31665–31672.
- (17) Hoang, L. P.; Nguyen, T. M. P.; Van, H. T.; Yilmaz, M.; Hoang, T. K.; Nguyen, Q. T.; Vi, T. M. H.; Nga, L. T. Q. Removal of Tetracycline from aqueous solution using composite adsorbent of ZnAl layered double hydroxide and bagasse biochar. *Environ. Technol. Innovation* **2022**, *28*, No. 102914.
- (18) Tang, J.; Ma, Y.; Cui, S.; Ding, Y.; Zhu, J.; Chen, X.; Zhang, Z. Insights on ball milling enhanced iron magnesium layered double oxides bagasse biochar composite for ciprofloxacin adsorptive removal from water. *Bioresour. Technol.* **2022**, *359*, No. 127468.
- (19) Zheng, D.; Wu, M.; Zheng, E.; Wang, Y.; Feng, C.; Zou, J.; Juan, M.; Bai, X.; Wang, T.; Shi, Y. Parallel adsorption of low concentrated ciprofloxacin by a CoFe-LDH modified sludge biochar. *J. Environ. Chem. Eng.* **2022**, *10* (5), No. 108381.
- (20) Tang, B.; Peng, G.; Luo, D.; Zhou, X. Preparation and Adsorption Properties of Soybean Dreg/Hydrocalumite Composites. *ACS Omega* **2021**, *6* (41), 27491–27500.
- (21) Chu, B.; Amano, Y.; Machida, M. Preparation of bean dreg derived N-doped activated carbon with high adsorption for Cr(VI). *Colloids Surf., A* **2020**, *586*, No. 124262.
- (22) Li, P.; Zhou, M.; Liu, H.; Lei, H.; Jian, B.; Liu, R.; Li, X.; Wang, Y.; Zhou, B. Preparation of green magnetic hydrogel from soybean residue cellulose for effective and rapid removal of copper ions from wastewater. *J. Environ. Chem. Eng.* **2022**, *10* (5), No. 108213.
- (23) Li, Y.; Li, Y.; Zang, H.; Chen, L.; Meng, Z.; Li, H.; Ci, L.; Du, Q.; Wang, D.; Wang, C.; et al. ZnCl<sub>2</sub>-activated carbon from soybean dregs as a high efficiency adsorbent for cationic dye removal: isotherm, kinetic, and thermodynamic studies. *Environ. Technol.* **2020**, *41* (15), 2013–2023.
- (24) Dante, R. C.; Chamorro-Posada, P.; Vázquez-Cabo, J.; Rubiños-López, Ó.; Sánchez-Árevalo, F. M.; Huerta, L.; Martín-Ramos, P.; Lartundo-Rojas, L.; Ávila-Vega, C. F.; Rivera-Tapia, E. D.; et al. Nitrogen-carbon graphite-like semiconductor synthesized from uric acid. *Carbon* **2017**, *121*, 368–379.
- (25) Wei, L.; Zietzschmann, F.; Rietveld, L. C.; van Halem, D. Fluoride removal by Ca-Al-CO<sub>3</sub> layered double hydroxides at environmentally-relevant concentrations. *Chemosphere* **2020**, *243*, No. 125307.

- (26) Peng, G.; Tang, B.; Zhou, X. Effect of Preparation Methods on the Adsorption of Glyphosate by Calcined Ca-Al Hydrotalcite. *ACS Omega* **2021**, *6* (24), 15742–15749.
- (27) Xiao, L.; Wang, Z.; Wang, D.; Lan, Y.; Kong, Q. Preparation of CaMgAl-calcined layered double hydroxides and application on the removal of phosphates. *Water Sci. Technol.* **2023**, *87* (3), 798–811.
- (28) dos Santos, G. E. d. S.; Lins, P. V. D. S.; Oliveira, L. M. T. D. M.; Silva, E. O. D.; Anastopoulos, I.; Erto, A.; Giannakoudakis, D. A.; Almeida, A. R. F. D.; Duarte, J. L. D. S.; Meili, L. Layered double hydroxides/biochar composites as adsorbents for water remediation applications: recent trends and perspectives. *J. Cleaner Prod.* **2021**, *284*, No. 124755.
- (29) Yuan, N.; Zhang, X.; Chen, T.; Xu, H.; Wang, Q. Fabricating Materials of Institute Lavoisier-53(Fe)/zeolite imidazolate framework-8 hybrid materials as high-efficiency and reproducible adsorbents for removing organic pollutants. *J. Colloid Interface Sci.* **2023**, *646*, 438–451.
- (30) Yao, B.; Luo, Z.; Du, S.; Yang, J.; Zhi, D.; Zhou, Y. Sustainable biochar/MgFe<sub>2</sub>O<sub>4</sub> adsorbent for levofloxacin removal: Adsorption performances and mechanisms. *Bioresour. Technol.* **2021**, *340*, No. 125698.
- (31) Qiu, B.; Tao, X.; Wang, H.; Li, W.; Ding, X.; Chu, H. Biochar as a low-cost adsorbent for aqueous heavy metal removal: A review. *J. Anal. Appl. Pyrolysis* **2021**, *155*, No. 105081.
- (32) Tan, X.; Liu, S.; Liu, Y.; Gu, Y.; Zeng, G.; Cai, X.; Yan, Z.; Yang, C.; Hu, X.; Chen, B. One-pot synthesis of carbon supported calcined-Mg/Al layered double hydroxides for antibiotic removal by slow pyrolysis of biomass waste. *Sci. Rep.* **2016**, *6* (1), 39691.
- (33) Oliveira, F. R.; Patel, A. K.; Jaisi, D. P.; Adhikari, S.; Lu, H.; Khanal, S. K. Environmental application of biochar: Current status and perspectives. *Bioresour. Technol.* **2017**, *246*, 110–122.
- (34) Singh, A. K.; Chaubey, A. K.; Kaur, I. Remediation of water contaminated with antibiotics using biochar modified with layered double hydroxide: Preparation and performance. *J. Hazard. Mater. Adv.* **2023**, *10*, No. 100286.
- (35) Zubair, M.; Ihsanullah, I.; Abdul Aziz, H.; Azmier Ahmad, M.; Al-Harthi, M. A. Sustainable wastewater treatment by biochar/layered double hydroxide composites: Progress, challenges, and outlook. *Bioresour. Technol.* **2021**, *319*, No. 124128.
- (36) Georgin, J.; Franco, D. S. P.; Ramos, C. G.; Picilli, D. G. A.; Lima, E. C.; Sher, F. A review of the antibiotic ofloxacin: Current status of ecotoxicology and scientific advances in its removal from aqueous systems by adsorption technology. *Chem. Eng. Res. Des.* **2023**, *193*, 99–120.
- (37) He, S.; Chen, Q.; Chen, G.; Shi, G.; Ruan, C.; Feng, M.; Ma, Y.; Jin, X.; Liu, X.; Du, C.; et al. N-doped activated carbon for high-efficiency ofloxacin adsorption. *Microporous Mesoporous Mater.* **2022**, *335*, No. 111848.
- (38) Hao, J.; Wu, L.; Lu, X.; Zeng, Y.; Jia, B.; Luo, T.; He, S.; Liang, L. A stable Fe/Co bimetallic modified biochar for ofloxacin removal from water: adsorption behavior and mechanisms. *RSC Adv.* **2022**, *12* (49), 31650–31662.
- (39) Huang, P.; Ge, C.; Feng, D.; Yu, H.; Luo, J.; Li, J.; Strong, P. J.; Sarmah, A. K.; Bolan, N. S.; Wang, H. Effects of metal ions and pH on ofloxacin sorption to cassava residue-derived biochar. *Sci. Total Environ.* **2018**, *616–617*, 1384–1391.
- (40) Zhang, J. Physical insights into kinetic models of adsorption. *Sep. Purif. Technol.* **2019**, *229*, No. 115832.
- (41) Ayawei, N.; Ebelegi, A. N.; Wankasi, D. Modelling and Interpretation of Adsorption Isotherms. *J. Chem.* **2017**, *2017*, No. 3039817.
- (42) Kaur, G.; Singh, N.; Rajor, A. Ofloxacin adsorptive interaction with rice husk ash: Parametric and exhausted adsorbent disposability study. *J. Contam. Hydrol.* **2021**, *236*, No. 103737.
- (43) Sharma, V.; Vinoth Kumar, R.; Pakshirajan, K.; Pugazhenth, G. Integrated adsorption-membrane filtration process for antibiotic removal from aqueous solution. *Powder Technol.* **2017**, *321*, 259–269.
- (44) Weng, X.; Cai, W.; Owens, G.; Chen, Z. Magnetic iron nanoparticles calcined from biosynthesis for fluoroquinolone antibiotic removal from wastewater. *J. Cleaner Prod.* **2021**, *319*, No. 128734.
- (45) Liu, Y.; Yuan, Y.; Wang, Z.; Wen, Y.; Liu, L.; Wang, T.; Xie, X. Removal of ofloxacin from water by natural ilmenite-biochar composite: A study on the synergistic adsorption mechanism of multiple effects. *Bioresour. Technol.* **2022**, *363*, No. 127938.
- (46) Santana, D. F.; de Melo, E. C. R.; Pessanha, M. L. G. S.; Guimarães, D. Removal of sulfate ions from aqueous solutions by precipitation using calcined hydrocalumite as a precipitating agent. *Int. J. Environ. Sci. Technol.* **2023**, *20* (4), 3801–3814.
- (47) de Sá, F. P.; Cunha, B. N.; Nunes, L. M. Effect of pH on the adsorption of Sunset Yellow FCF food dye into a layered double hydroxide (CaAl-LDH-NO<sub>3</sub>). *Chem. Eng. J.* **2013**, *215–216*, 122–127.
- (48) Gao, B.; Li, P.; Yang, R.; Li, A.; Yang, H. Investigation of multiple adsorption mechanisms for efficient removal of ofloxacin from water using lignin-based adsorbents. *Sci. Rep.* **2019**, *9* (1), 637.
- (49) Deng, S.; Long, J.; Dai, X.; Wang, G.; Zhou, L. Simultaneous Detection and Adsorptive Removal of Cr(VI) Ions by Fluorescent Sulfur Quantum Dots Embedded in Chitosan Hydrogels. *ACS Appl. Nano Mater.* **2023**, *6* (3), 1817–1827.
- (50) Wu, H.; Gao, H.; Yang, Q.; Zhang, H.; Wang, D.; Zhang, W.; Yang, X. Removal of Typical Organic Contaminants with a Recyclable Calcined Chitosan-Supported Layered Double Hydroxide Adsorbent: Kinetics and Equilibrium Isotherms. *J. Chem. Eng. Data* **2018**, *63* (1), 159–168.